

Relic Density of Neutrinos with Primordial Asymmetries

Sergio Pastor,¹ Teguayco Pinto,¹ and Georg G. Raffelt²

¹*Institut de Física Corpuscular (CSIC-Universitat de València), Ed. Instituts d'Investigació, Apt. 22085, 46071 València, Spain*

²*Max-Planck-Institut für Physik (Werner-Heisenberg-Institut), Föhringer Ring 6, 80805 München, Germany*

(Received 27 August 2008; published 19 June 2009)

We study flavor oscillations in the early Universe, assuming primordial neutrino-antineutrino asymmetries. Including collisions and pair processes in the kinetic equations, we not only estimate the degree of flavor equilibration, but for the first time also kinetic equilibration among neutrinos and with the ambient plasma. Typically, the restrictive big-bang nucleosynthesis bound on the $\nu_e \bar{\nu}_e$ asymmetry indeed applies to all flavors as claimed in the previous literature, but fine-tuned initial asymmetries always allow for a large surviving neutrino excess radiation that may show up in precision cosmological data.

DOI: 10.1103/PhysRevLett.102.241302

PACS numbers: 26.35.+c, 14.60.Pq, 98.70.Vc

Introduction.—The state of the hot medium in the early Universe before and around big-bang nucleosynthesis (BBN) is fixed by a small number of cosmological parameters, most importantly the baryon abundance that nowadays is measured most accurately with precision cosmological data. In addition, there are three unknown neutrino asymmetries, one for each flavor, that modify the cosmic neutrino density and, for the case of the $\nu_e \bar{\nu}_e$ asymmetry, influence β reactions of the form $e^- + p \leftrightarrow n + \nu_e$ and $e^+ + n \leftrightarrow p + \bar{\nu}_e$, and thus the primordial ^4He abundance [1–7].

It is often assumed that sphalerons equilibrate the lepton and baryon asymmetries, implying that all neutrino asymmetries are of order 10^{-9} or smaller, leaving no observable trace. On the other hand, sphalerons have never been observed, so a cosmic neutrino asymmetry would raise fundamental questions about both electroweak physics and the early Universe. In any event, improving observational information on neutrino asymmetries is part of the ongoing effort to determine all cosmological parameters with increasing accuracy.

Neutrino oscillations driven by the “solar” and “atmospheric” mass differences $\Delta m_{\text{sol}}^2 = 7.65_{-0.40}^{+0.46} \times 10^{-5} \text{ eV}^2$ and $\Delta m_{\text{atm}}^2 = \pm 2.40_{-0.22}^{+0.24} \times 10^{-3} \text{ eV}^2$ and by the large mixing angles $\sin^2 \theta_{12} = 0.30_{-0.03}^{+0.05}$ and $\sin^2 \theta_{23} = 0.50_{-0.11}^{+0.13}$ are now established, whereas the third angle is constrained by $\sin^2 \theta_{13} < 0.04$ and could actually vanish. (2σ ranges, taken from Ref. [8].) In the early Universe, flavor conversions are suppressed by large matter effects. Oscillations driven by Δm_{atm}^2 begin only at $T \sim 10 \text{ MeV}$, whereas those driven by Δm_{sol}^2 begin as late as 3 MeV , still early enough to achieve strong flavor conversions before BBN [9–12]. Therefore, all flavors must have similar asymmetries at BBN and the restrictive limit on the ν_e degeneracy parameter, conservatively $-0.04 \lesssim \xi_{\nu_e} \lesssim 0.07$ [4], seemingly applies to all flavors, unless oscillations are blocked, for instance by a hypothetical neutrino-majoron coupling [13].

Based on this reasoning it was often concluded that primordial neutrino asymmetries could not cause a signifi-

cant increase of the cosmic neutrino density without violating the BBN bound on ξ_{ν_e} . Assuming that neutrinos indeed reach perfect kinetic and chemical equilibrium, the possible increase of the cosmic radiation density is small, $\Delta N_{\text{eff}} = \frac{30}{7} (\xi_{\nu_e}/\pi)^2 + \frac{15}{7} (\xi_{\nu_e}/\pi)^4 \lesssim 0.006$. Here, the usual “effective number of neutrino families” measures the cosmic radiation density, after e^+e^- annihilation, by $\rho_{\text{rad}}/\rho_{\gamma} = 1 + (7/8)(4/11)^{4/3} N_{\text{eff}}$.

We stress, however, that Refs. [10–12] do not claim that neutrinos after flavor conversions follow Fermi-Dirac distributions in terms of a common degeneracy parameter and the temperature of the ambient plasma. References [11,12] showed that, if $\theta_{13} = 0$ and if one ignores collisions, synchronized MSW-like flavor conversions driven by Δm_{sol}^2 and θ_{12} achieve comparable $\nu \bar{\nu}$ asymmetries among all flavors, but this is not the same as kinetic and chemical equilibrium. Reference [10] included collisions in a schematic way, showing that the coherence among flavors was efficiently destroyed. However, the transfer of entropy to the electromagnetic plasma was not considered and the final neutrino distributions not studied.

If all initial asymmetries have the same sign, oscillations alone are enough to achieve approximate flavor equipartition and the BBN limits on the $\nu_e \bar{\nu}_e$ asymmetry will apply to all flavors. A dangerous case arises, however, if one begins with opposite asymmetries in two flavors. Oscillations, with or without collisions, will achieve approximate flavor equipartition separately among neutrinos and antineutrinos, so in the end all asymmetries vanish. On the other hand, the original excess radiation remains. The efficiency of $\nu \bar{\nu} \rightarrow e^+e^-$ entropy transfer determines if the BBN limits on the $\nu_e \bar{\nu}_e$ asymmetry still preclude a large ΔN_{eff} . The main point of our paper is to study this case that was not covered in previous treatments [10–12].

Numerical approach.—We describe neutrino distributions by 3×3 matrices in flavor space \mathcal{Q}_{p} for each mode. The diagonal elements are the usual occupation numbers whereas the off-diagonal ones encode phase information. We need to solve the equations of motion (EOMs) [14,15]

$$i\dot{\varrho}_{\mathbf{p}} = [\Omega_{\mathbf{p}}, \varrho_{\mathbf{p}}] + C(\varrho_{\mathbf{p}}, \bar{\varrho}_{\mathbf{p}}) \quad (1)$$

and similar for the antineutrino matrices $\bar{\varrho}_{\mathbf{p}}$. The first term on the right-hand side (a commutator expression) describes oscillations with

$$\Omega_{\mathbf{p}} = \frac{M^2}{2p} + \sqrt{2}G_F \left(-\frac{8p}{3m_w^2} \mathbf{E} + \varrho - \bar{\varrho} \right), \quad (2)$$

where $p = |\mathbf{p}|$, M is the neutrino mass matrix, $\varrho = \int \varrho_{\mathbf{p}} d^3\mathbf{p} / (2\pi)^3$ and similar for $\bar{\varrho}$. The small baryon density implies that the dominant matter term in the oscillation matrix is equal for neutrinos and antineutrinos, where \mathbf{E} is the 3×3 flavor matrix of charged-lepton energy densities [14,16]. The matrix $\bar{\Omega}_{\mathbf{p}}$ for antineutrinos is the same with $M^2/2p \rightarrow -M^2/2p$. The term proportional to $\varrho - \bar{\varrho}$ is responsible for synchronized oscillations [10–12].

Solving these EOMs with the full collision terms $C(\varrho_{\mathbf{p}}, \bar{\varrho}_{\mathbf{p}})$ is numerically challenging and not necessary for a first exploratory study. Collisions have two main effects: They break the phase coherence of mixed flavor states and they create or destroy neutrino pairs. The first effect is efficiently implemented with p -dependent damping factors for those $\varrho_{\mathbf{p}}$ elements that are off-diagonal in the weak-interaction basis. Here we follow exactly the earlier work of Dolgov *et al.* [10] in that we use the damping factors spelled out in Eqs. (60) and (61) of Ref. [15]. Essentially one assumes that neutrinos collapse into weak-interaction eigenstates each time they interact in a process that distinguishes among flavors [17].

The crucial new ingredients are collisions and pair processes for the diagonal $\varrho_{\mathbf{p}}$ elements, allowing the neutrino distributions to achieve equilibrium with the ambient plasma. With small modifications we here use an existing numerical code [18] where the collision integrals are solved without approximation, using the same approach as Ref. [19]. For example, we obtain exact Fermi-Dirac distributions if the relaxation time is large enough.

So in our implementation the diagonal elements change by collisions and oscillations, whereas the off-diagonal elements change by oscillations and damping. We have checked that the damping factors of Ref. [15] and the collision rates used in the code [18] are consistent with each other. Changing the damping factors by as much as a factor of 2 has only a minimal impact on the final ΔN_{eff} . Of course, our combined treatment of oscillations, damping of flavor coherence, and collisions and pair processes is only approximate and would be questionable if one were to aim at a precision determination of ΔN_{eff} . However, our relatively simple extension of existing tools provides a first reasonable estimate of the surviving ΔN_{eff} .

Opposite equal asymmetries.—Our main example is the “dangerous case” of two large but opposite initial asymmetries. To be specific, we first consider an exactly vanishing global lepton asymmetry. The initial asymmetry in one flavor ν_{α} , defined in analogy to the baryon asymmetry, is

$$\eta_{\nu_{\alpha}} = \frac{n_{\nu_{\alpha}} - n_{\bar{\nu}_{\alpha}}}{n_{\gamma}} = \frac{1}{12\zeta(3)} (\pi^2 \xi_{\nu_{\alpha}} + \xi_{\nu_{\alpha}}^3). \quad (3)$$

A vanishing global asymmetry requires for the initial degeneracy parameters $2(\pi^2 \xi_{\nu_x} + \xi_{\nu_x}^3) + (\pi^2 \xi_{\nu_e} + \xi_{\nu_e}^3) = 0$.

In Fig. 1 we show the evolution of ρ_{ν}/ρ_{γ} , properly normalized so that it corresponds to N_{eff} at early and late times, first for the baseline case without asymmetries (dotted lines). The fast drop of ρ_{ν}/ρ_{γ} at $T \sim 0.2$ MeV represents photon heating by e^+e^- annihilation. At late times the dotted lines end at $N_{\text{eff}} = 3.046$ instead of 3 because of residual neutrino heating [18].

Next we show (solid lines) the evolution for our main example where $\xi_{\nu_x} = -0.64$ and $\xi_{\nu_e} = 1.17$, corresponding to an initial value $N_{\text{eff}} = 4.0$. The neutrino mass differences and θ_{23} are fixed to their best-fit values. In the upper panel we assume $\theta_{13} = 0$ and for the upper curve also $\theta_{12} = 0$ (no oscillations), leading to an unchanged final $N_{\text{eff}} = 4.0$. The bottom curve is for $\sin^2\theta_{12} = 0.5$ (maximal mixing), showing that at $T_{\gamma} \sim 3$ MeV the neutrino density depletes relative to photons, when oscillations driven by Δm_{sol}^2 begin and the flavour asymmetries are reduced. The main effect of collisions is to keep the neutrino spectra closer to their equilibrium form:

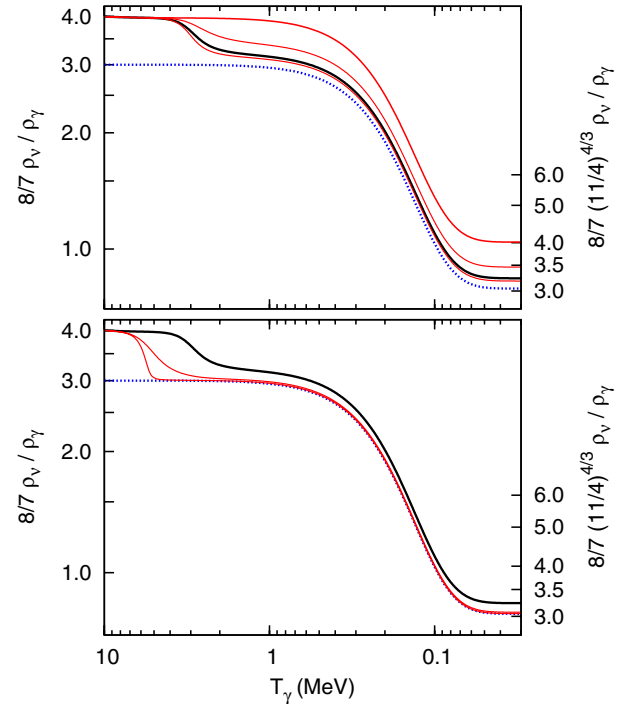


FIG. 1 (color online). Evolution of the neutrino energy density. The vertical axis is marked with N_{eff} , left before e^+e^- annihilation, right afterwards. Dotted lines: Baseline case without asymmetries. Top panel: $\theta_{13} = 0$, the solid lines correspond to $\sin^2\theta_{12} = 0, 0.1, 0.3, \text{ and } 0.5$ from top to bottom. Bottom panel: $\sin^2\theta_{12} = 0.3$, the top solid curve is $\sin^2\theta_{13} = 0$, while the other solid curves correspond to $\sin^2\theta_{13} = 0.04$ with normal (top) and inverted (bottom) hierarchy.

Physically the excess of entropy is transferred from neutrinos to the electromagnetic plasma, cooling the former and heating the latter. Practically the same behavior is found for the next curve representing $\sin^2\theta_{12} = 0.3$, the experimental best fit, where in the end $N_{\text{eff}} = 3.24$. A further curve is shown for the value $\sin^2\theta_{12} = 0.1$, remaining far from equilibrium until the end. In the bottom panel we use the measured $\sin^2\theta_{12} = 0.3$ and repeat the case $\theta_{13} = 0$ (top curve). The other two curves are for $\sin^2\theta_{13} = 0.04$, near the experimental limit, for the normal and inverted hierarchies.

As expected, a nonvanishing θ_{13} together with Δm_{atm}^2 drives the system towards equilibrium at a time when collisions are still efficient. In our numerical example, a significant deviation from equilibrium survives only for a very small θ_{13} . In this case the outcome depends on θ_{12} as found in the original studies [10–12]. A small θ_{12} does not lead anywhere close to flavor equilibrium, a large value leads to near-equilibrium.

For $\theta_{13} = 0$ and $\sin^2\theta_{12} = 0.3$ we show the final ν_e and $\bar{\nu}_e$ energy spectra in Fig. 2. We compare them with Fermi-Dirac spectra that produce the same $\nu_e\bar{\nu}_e$ asymmetry and the same energy density $\rho_{\nu_e} + \rho_{\bar{\nu}_e}$, implying $\xi_{\nu_e} = 0.185$ and a T_{ν_e} only 5% higher relative to the equilibrium value. These spectra are much closer to kinetic equilibrium than expected.

Asymmetry scan.—Next we study the final deviation from equilibrium for a range of initial asymmetries $0 \leq \xi_{\nu_e} \leq 3$, assuming a vanishing global asymmetry as before. In Fig. 3 we show the final outcome in terms of the residual excess radiation density ΔN_{eff} and ξ_{ν_e} and T_{ν_e} chosen for a Fermi-Dirac distribution that approximates the final ν_e and $\bar{\nu}_e$ spectra such that we reproduce the numerical asymmetry and energy density. We show these results for the experimental best-fit value $\sin^2\theta_{12} = 0.3$ and for $\theta_{13} = 0$ as well as $\sin^2\theta_{13} = 0.04$.

Qualitatively we confirm that kinetic equilibrium is rather good in that the final neutrino temperature is close

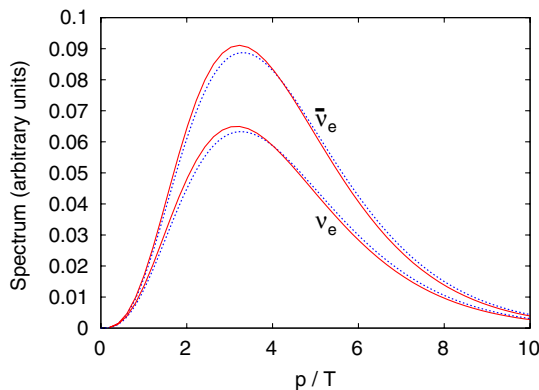


FIG. 2 (color online). Final ν_e and $\bar{\nu}_e$ spectra for $\theta_{13} = 0$ and $\sin^2\theta_{12} = 0.3$. The dotted lines are Fermi-Dirac spectra producing the same $\nu_e\bar{\nu}_e$ asymmetry and the same energy density $\rho_{\nu_e} + \rho_{\bar{\nu}_e}$.

to what it should be in equilibrium. Moreover, we also find that the value of θ_{13} is crucial in determining how close the system comes to equilibrium, which, however, is never perfect for any value of θ_{13} . If $\sin^2\theta_{13} \lesssim 10^{-3}$, the outcome is very close to a vanishing θ_{13} .

We note that for large initial ξ_{ν_e} the final electron neutrino degeneracy can be so large that it is excluded by BBN. However, we are not bound to the assumption of an initially vanishing global asymmetry, but we can use slightly more negative initial ξ_{ν_x} values such that the final ξ_{ν_e} is pulled into the range allowed by BBN, yet a significant excess radiation density survives as shown in Fig. 3, being quite similar to ΔN_{eff} for the simple case of a vanishing global asymmetry. In other words, up to small adjustments of initial conditions, the simple case of a vanishing global asymmetry gives us a fair idea of a possible surviving residual radiation density.

No initial $\nu_e\bar{\nu}_e$ asymmetry.—Another initial configuration for a vanishing global asymmetry is $\xi_{\nu_e} = 0$ and $\xi_{\nu_\mu} = -\xi_{\nu_\tau}$. If the latter are exactly equal but opposite,

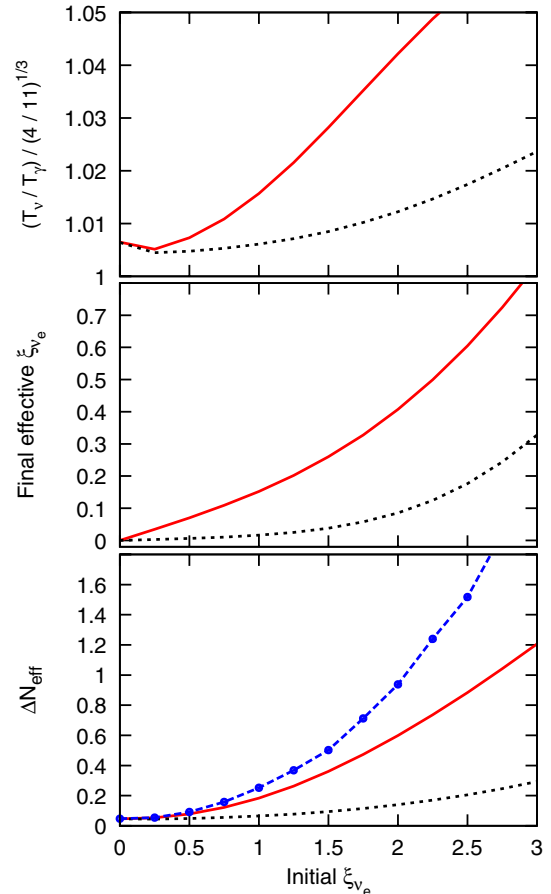


FIG. 3 (color online). Parameters for the final ν_e and $\bar{\nu}_e$ spectra as well as the final ΔN_{eff} as a function of the initial ξ_{ν_e} . The solid lines correspond to $\theta_{13} = 0$, the dotted lines to $\sin^2\theta_{13} = 0.04$. In the bottom panel, the dashed line is the surviving ΔN_{eff} when the final ξ_{ν_e} is in the range allowed by BBN.

$\nu_\mu\nu_\tau$ oscillations driven by Δm_{atm}^2 and θ_{23} are suppressed by neutrino-neutrino interactions in that the synchronized oscillation frequency vanishes exactly [10]. However, oscillations driven by Δm_{sol}^2 and θ_{12} achieve approximate equilibrium, the transformations beginning at $T \sim 3$ MeV as before. We have not studied this case in detail because it is numerically more challenging. We note that “blocking” the $\nu_\mu\nu_\tau$ oscillations requires a very precise cancellation and thus a more special case than before where an exactly vanishing global asymmetry was only a choice of convenience.

Conclusions.—The first studies of primordial neutrino flavor equilibration were concerned with the role of the solar neutrino mixing parameters and found that approximate global flavor equilibrium is only achieved for the now-established “large mixing angle solution” [10–12]. While this conclusion is correct, we here stress that it must not be over interpreted. Oscillations driven by the solar parameters take place so late ($T \sim 3$ MeV) that neither perfect flavor equilibrium nor thermal equilibrium with the ambient plasma is achieved, although a large value for θ_{13} helps to come closer because flavor transformations begin earlier. (If $\sin^2\theta_{13} \lesssim 10^{-3}$ it plays no significant role.) For $\theta_{13} = 0$ we have constructed an explicit example with nearly equal but opposite asymmetries between ν_e and the other flavors such that the BBN limit on ξ_{ν_e} is satisfied, yet a large ΔN_{eff} survives.

Precision cosmology has advanced in such strides that today one can derive nontrivial bounds on the cosmic radiation density that however still allow for ΔN_{eff} of a few [20–25]. It is conceivable that in future one can do much better and constrain or detect a value of ΔN_{eff} significantly smaller than unity [26–30], for instance with very precise CMB data from Planck. Such results remain complementary to BBN limits on ξ_{ν_e} . If precision cosmology were to turn up a nonvanishing ΔN_{eff} , it could be a remnant of a primordial neutrino asymmetry, although the exact interpretation would strongly depend on θ_{13} . In this sense, future measurements of θ_{13} are important for the interpretation of cosmological precision data.

In summary, the established neutrino mixing parameters together with BBN constraints on ξ_{ν_e} typically assure that the surviving excess radiation density is immeasurably small, in agreement with the previous literature. However, imperfect kinetic and chemical equilibrium achieved by the solar mixing parameters allows for exceptions. In particular, large but opposite primordial asymmetries of two flavors can be fine-tuned such that the ξ_{ν_e} limit is respected, yet a large excess radiation density survives with ΔN_{eff} of order unity or larger that may be detectable in future cosmological precision data.

We thank Y. Y. Y. Wong for comments on the manuscript. This work was partly supported by the DFG (Germany) grant TR-27 “Neutrinos and Beyond,” the Cluster of Excellence “Origin and Structure of the Universe,” the European Union (RT Network MRTN-CT-

2004-503369), and the Spanish grants FPA2005-01269/FPA2008-00319 (MICINN) and BEST/2008/164 (Generalitat Valenciana). T.P. was supported by a Spanish FPU grant. S.P. thanks the MPI for Physics in Munich for hospitality and financial support for his visit when this work was completed.

-
- [1] H. S. Kang and G. Steigman, Nucl. Phys. **B372**, 494 (1992).
 - [2] S. Sarkar, Rep. Prog. Phys. **59**, 1493 (1996).
 - [3] S. Esposito *et al.*, Nucl. Phys. **B590**, 539 (2000).
 - [4] P. D. Serpico and G. G. Raffelt, Phys. Rev. D **71**, 127301 (2005).
 - [5] O. Pisanti *et al.*, Comput. Phys. Commun. **178**, 956 (2008).
 - [6] V. Simha and G. Steigman, J. Cosmol. Astropart. Phys. **08** (2008) 011.
 - [7] F. Iocco *et al.*, Phys. Rep. **472**, 1 (2009).
 - [8] T. Schwetz, M. Tórtola, and J. W. F. Valle, New J. Phys. **10**, 113011 (2008).
 - [9] C. Lunardini and A. Yu. Smirnov, Phys. Rev. D **64**, 073006 (2001).
 - [10] A. D. Dolgov *et al.*, Nucl. Phys. **B632**, 363 (2002).
 - [11] Y. Y. Y. Wong, Phys. Rev. D **66**, 025015 (2002).
 - [12] K. N. Abazajian, J. F. Beacom, and N. F. Bell, Phys. Rev. D **66**, 013008 (2002).
 - [13] A. D. Dolgov and F. Takahashi, Nucl. Phys. **B688**, 189 (2004).
 - [14] G. Sigl and G. Raffelt, Nucl. Phys. **B406**, 423 (1993).
 - [15] B. H. McKellar and M. J. Thomson, Phys. Rev. D **49**, 2710 (1994).
 - [16] D. Nötzold and G. Raffelt, Nucl. Phys. **B307**, 924 (1988).
 - [17] G. Raffelt, G. Sigl, and L. Stodolsky, Phys. Rev. Lett. **70**, 2363 (1993); **98**, 069902(E) (2007).
 - [18] G. Mangano *et al.*, Nucl. Phys. **B729**, 221 (2005).
 - [19] A. D. Dolgov, S. H. Hansen, and D. V. Semikoz, Nucl. Phys. **B503**, 426 (1997).
 - [20] G. Mangano *et al.*, J. Cosmol. Astropart. Phys. **03** (2007) 006.
 - [21] J. Hamann, S. Hannestad, G. G. Raffelt, and Y. Y. Y. Wong, J. Cosmol. Astropart. Phys. **08** (2007) 021.
 - [22] F. de Bernardis, A. Melchiorri, L. Verde, and R. Jiménez, J. Cosmol. Astropart. Phys. **03** (2008) 020.
 - [23] E. Komatsu *et al.* (WMAP Collaboration), Astrophys. J. Suppl. Ser. **180**, 330 (2009).
 - [24] L. A. Popa and A. Vasile, J. Cosmol. Astropart. Phys. **06** (2008) 028.
 - [25] K. Ichikawa, T. Sekiguchi, and T. Takahashi, Phys. Rev. D **78**, 083526 (2008).
 - [26] S. Bashinsky and U. Seljak, Phys. Rev. D **69**, 083002 (2004).
 - [27] S. Hannestad, H. Tu, and Y. Y. Y. Wong, J. Cosmol. Astropart. Phys. **06** (2006) 025.
 - [28] L. Perotto *et al.*, J. Cosmol. Astropart. Phys. **10** (2006) 013.
 - [29] A. Friedland, K. M. Zurek, and S. Bashinsky, arXiv:0704.3271.
 - [30] J. Hamann, J. Lesgourgues, and G. Mangano, J. Cosmol. Astropart. Phys. **03** (2008) 004.